THE UNIVERSITY *of* EDINBURGH

Edinburgh Research Explorer

Patterns of genomic change in residual disease after neoadjuvant chemotherapy for estrogen receptor-positive and HER2-negative breast cancer

Citation for published version:
Chatzipli, A, Bonnefoi, H, Macgrogan, G, Sentis, J, Cameron, D, Poncet, C, Abadie-lacourtoisie, S, Bodmer, A, Brain, E, Cufer, T, Campone, M, Luporsi, E, Moldovan, C, Petit, T, Piccart, M, Priou, F, Senkus, E, Zaman, K & Iggo, R 2021, 'Patterns of genomic change in residual disease after neoadjuvant chemotherapy for estrogen receptor-positive and HER2-negative breast cancer', *British Journal of Cancer*. https://doi.org/10.1038/s41416-021-01526-3

Digital Object Identifier (DOI):
10.1038/s41416-021-01526-3

Link:
Link to publication record in Edinburgh Research Explorer

Document Version:
Peer reviewed version

Published In:
British Journal of Cancer

Publisher Rights Statement:
This is a pre-copyedited, author-produced version of an article accepted for publication in British Journal of Cancer following peer review. The version of record "Patterns of genomic change in residual disease after neoadjuvant chemotherapy for estrogen receptor-positive and HER2-negative breast cancer" is available online at: https://doi.org/10.1038/s41416-021-01526-3

General rights
Copyright for the publications made accessible via the Edinburgh Research Explorer is retained by the author(s) and / or other copyright owners and it is a condition of accessing these publications that users recognise and abide by the legal requirements associated with these rights.

Take down policy
The University of Edinburgh has made every reasonable effort to ensure that Edinburgh Research Explorer content complies with UK legislation. If you believe that the public display of this file breaches copyright please contact openaccess@ed.ac.uk providing details, and we will remove access to the work immediately and investigate your claim.

Download date: 13. May. 2024

Patterns of genomic change in residual disease after neo-adjuvant chemotherapy for estrogen receptor positive and HER2 negative breast cancer

Aikaterini Chatzipli (1) (*)
Hervé Bonnefoi (2) (*)
Gaetan MacGrogan (2)
Julie Sentis (2)
David Cameron (3)
Coralie Poncet (4)
EORTC 10994/BIG 1-00 Consortium (**)
Richard Iggo (2)

Affiliations

(1) Wellcome Sanger Institute, Cambridge, United Kingdom
(2) Institut Bergonié, INSERM U1218, University of Bordeaux, France
(3) University of Edinburgh, UK
(4) EORTC Data Centre, Brussels, Belgium

(*) These authors contributed equally
(**) A list of authors and their affiliations appears at the end of the paper

Corresponding author

Richard Iggo, ORCID 0000-0002-8822-9111
Richard.Iggo@u-bordeaux.fr

Key words: breast cancer, neoadjuvant chemotherapy, next generation sequencing, clonal evolution

Abstract

Background

Treatment of patients with residual disease after neo-adjuvant chemotherapy for breast cancer is an unmet clinical need. We hypothesised that tumour subclones showing expansion in residual disease after chemotherapy would contain mutations conferring drug resistance.

Methods

We studied estrogen receptor and/or progesterone receptor-positive, HER2-negative tumours from 42 patients in the EORTC 10994/BIG 00-01 trial who failed to achieve pathological complete response. Genes commonly mutated in breast cancer were sequenced in pre and post-treatment samples.

Results

Oncogenic driver mutations were commonest in PIK3CA (38% of tumours), GATA3 (29%), CDH1 (17%), TP53 (17%) and CBFB (12%); and amplification was commonest for CCND1 (26% of tumours) and FGFR1 (26%). The variant allele fraction frequently changed after treatment, indicating that subclones had expanded and contracted, but there were changes in both directions for all of the commonly mutated genes.

Conclusions

We found no evidence that expansion of clones containing recurrent oncogenic driver mutations is responsible for resistance to neoadjuvant chemotherapy. The persistence of classic oncogenic mutations in pathways for which targeted therapies are now available highlights their importance as drug targets in patients who have failed chemotherapy but provides no support for a direct role of driver oncogenes in resistance to chemotherapy.

ClinicalTrials.gov: EORTC 10994/BIG 1-00 Trial registration number NCT00017095.

Background

Neoadjuvant chemotherapy (NAC) before loco-regional treatment is widely used in patients with large operable or locally advanced breast cancers. Several trials have demonstrated that patients without residual invasive disease in the surgical specimen (primary breast tumour and lymph nodes) after neoadjuvant chemotherapy have a low risk of relapse [1-3] and trials aiming to de-escalate therapy in this group of patients are ongoing. On the other hand, patients with residual invasive tumour after neoadjuvant chemotherapy have at least a 25% risk of invasive relapse within 5 years [1-4]. This high risk of relapse is observed in all molecular breast cancer subtypes despite the systematic use of adjuvant hormonal therapy in luminal tumours and trastuzumab in HER2-positive tumours [1-4].

Based on these data, treatment of patients with residual invasive disease after NAC should be considered as an unmet clinical need. Several studies have been conducted or are ongoing to assess the clinical impact of additional post-neoadjuvant treatments in these patients after standard neoadjuvant treatment. This approach has been successful in two recently published phase III studies. A first study conducted in luminal HER2-negative and triple negative breast cancers (TNBC) compared observation to capecitabine for six to eight cycles [5]. This trial demonstrated a survival advantage in the overall population which was more pronounced in the TNBC group. A second study conducted in HER2-positive tumours compared standard treatment with trastuzumab for 1 year to trastuzumab emtansine (T-DM1) for the same duration [6]. This study demonstrated a halving of the risk of invasive relapse with T-DM1 as compared to continued trastuzumab.

Although this "one size fits all" post-neoadjuvant chemotherapy strategy in patients with residual disease has been successful in these two phase III studies, a large proportion of patients will still relapse. A personalised post-neoadjuvant chemotherapy strategy based on genomic analysis of residual disease could have two important advantages. First, tumour cells in the residual tumour after neoadjuvant chemotherapy are by definition resistant to this treatment. We would expect genomic aberrations conferring resistance to be more easily identified in samples taken after treatment had eliminated the drug-sensitive cells present in the primary tumour. Second, genomic analysis of tumour cells in residual disease could identify de novo mutations that were not present before chemotherapy. These mutations might create new therapeutic opportunities. A previous study focusing on residual disease after NAC for TNBC identified genetic alterations which could potentially be targeted in 90% of the tumours [7] but there was no evidence that these were de novo mutations selected by the treatment. Another study on TNBC and one including multiple subtypes also failed to identify any recurrent changes after treatment [8,9].

37 In this study, we chose to focus on luminal HER2-negative tumours because these tumours are the
38 most frequent and account for the largest number of breast cancer deaths. We therefore believe
39 that the greatest unmet need lies in this group. The genomic landscape of luminal (ER positive and
40 HER2 negative) tumours has been reported in the literature both before any systemic therapy [10]
41 and in the metastatic setting [11]. However, to our knowledge, there are no data available from this
42 group of tumours after NAC. We were particularly interested in the possibility that post-treatment
43 samples would show expansion of clones containing mutations that can be targeted by therapies
44 that have shown efficacy in patients with metastatic disease, such as PIK3CA mutations [12],
45 BRCA1/2 mutations [13] and AKT1 mutations [14].
46
47 Formally, the primary objective of this study was to discover mechanisms of resistance to
48 neoadjuvant chemotherapy in luminal breast cancer by identifying genetic changes in subclones
49 showing clonal expansion after treatment. To identify clonal expansion we analysed variant allele
50 fractions (VAF) in matched samples before and after chemotherapy from 42 patients with luminal
51 (ER and/or PgR positive) HER2-negative breast cancer who did not achieve a pathological
52 complete response (pCR) after neoadjuvant therapy within the EORTC 10994/BIG1-00 trial [15].
53
54 The neoadjuvant design of the original 10994 study means we can compare pre-treatment with
55 post-treatment samples to identify changes potentially selected by the treatment. This approach
56 reduces confounding by germline mutations. To reduce the background from passenger mutations
57 we restricted the analysis to a panel of genes that are known to be mutated in breast cancer.
58
59

60 **Patients and methods**

61 **Study design, treatment and eligibility**

62 This is an ancillary study of the EORTC 10994/BIG 1-00 trial which randomized patients between
63 six cycles of a non-taxane regimen (5-fluorouracil, epirubicin, cyclophosphamide) and a taxane-
64 based regimen (docetaxel for three cycles followed by epirubicin + docetaxel for three cycles) all
65 given before primary surgery [15]. Eligible patients were women aged less than 71 years with
66 histologically-proven invasive carcinoma of the breast suitable for neoadjuvant chemotherapy, with
67 any large operable or locally advanced/inflammatory breast cancer. The trial was approved by
68 national and/or local ethics committees in all participating centres. Patients gave signed informed
69 consent at the time of enrolment for the original EORTC 10994 study.

70 For the sub-study that is the subject of this report, we have selected patients in a subgroup
71 of the initial population of 1856 based on the following eligibility criteria: (1) patients eligible for the
72 main p53 trial; (2) patients who gave informed consent for optional research on tumour samples;
73 (3) luminal tumours (ER and/or PgR positive) and HER2-negative based on assessment by local
74 laboratory; (4) patients who received at least one cycle of neo-adjuvant chemotherapy and who did
75 not receive radiotherapy before surgery; (5) non pCR after neoadjuvant chemotherapy; (6) Pre-
76 and post-chemotherapy samples with more than 50% invasive tumour cells and 250-300 ng DNA
77 available (for details see Sup Table 1 and the CONSORT diagram in Sup Fig 1).

78

79 **Objectives**

80 The primary objective was to discover mechanisms of resistance to NAC by identifying recurrent
81 genetic changes in subclones showing clonal expansion after treatment. We defined clonal
82 expansion as a significant change by Fisher test in the variant allele fraction (VAF) after treatment.
83 The secondary objectives were: 1. To describe the mutational landscape of all the samples
84 (number of coding mutations, number of driver mutations, type of mutations), 2. To identify
85 changes in the mutational landscape after NAC (VAF changes in driver oncogenes, copy number
86 changes in driver oncogenes), 3. To document the expansion and contraction of subclones after
87 NAC.

88

89 **Tumour samples and pathology assessment**

90 Tumour biopsies were taken with a 14G trucut needle before starting neoadjuvant chemotherapy.
91 Some of these biopsies were fixed in formalin and embedded in paraffin (FFPE) as part of routine
92 assessment, the remaining biopsies were frozen as part of the mandatory procedure in the original
93 EORTC 10994/BIG 1-00 trial. Grade, ER, PR, and HER2 status were assessed by local
94 pathologists from a biopsy taken at diagnosis before starting neoadjuvant chemotherapy and
95 prospectively recorded in the case report form. ER and PR, assessed by immunohistochemistry
96 (IHC), were reported as positive or negative according to each centre’s local definition. HER2

negativity was defined as either absence of HER2 gene amplification by fluorescent in situ hybridization or a score of 0-1+ by IHC. Pathological response after completion of neoadjuvant chemotherapy was assessed by local pathologists on formalin fixed samples taken during surgical resection of the residual tumour. Non pCR cases were defined as patients with residual invasive disease in the primary tumour and/or in the nodes as reported by the local pathologist.

We collected and centralized in Bordeaux both frozen pre-chemotherapy samples and FFPE post-chemotherapy samples taken during surgery. We have summarised in Sup Fig 1 how the 42 patients were selected from the initial population of 1856 patients, of whom 499 with ER and/or PgR positive and HER2-negative tumours were theoretically eligible for this substudy. We initially considered performing NGS on pre-chemotherapy FFPE trucut biopsies but a pilot study showed that NGS was not feasible with these samples. Post-chemotherapy samples were taken from surgical specimens and formalin fixed. H&E sections were examined to estimate tumour cellularity. All of these samples were centrally reviewed by a board-certified pathologist (GMG) to estimate the tumour cell content and to mark regions in the FFPE samples for DNA extraction. The samples qualified if more than 50% of the cells in the biopsy sample were invasive cancer cells.

DNA extraction and sequencing

In Bordeaux (Bergonié Institute), DNA was purified on Qiagen columns after proteinase K digestion of the pre-chemotherapy frozen samples. For post-chemotherapy FFPE samples, one or two 1 mm diameter cores of 0.5 to 1 mm thickness, depending on the material available, were taken and DNA was extracted with the GeneRead DNA FFPE kit (ref 180134 Qiagen, Hilden, Germany). DNA concentration was measured by Qubit and tubes containing 250-300ng of DNA at >30ng/ul were sent to the Wellcome Sanger Institute (WSI). An electronic manifest linking barcodes to EORTC 10994 Sample IDs was sent to WSI with the tubes.

In Cambridge (WSI), samples were further anonymised with replacement of the EORTC Sample ID with a Sanger ID. 100 SNPs were used to check that pre and post-treatment samples were derived from the same patient. Genomic DNA was quality controlled and 200 ng was used for library preparation. DNA was sheared to an average fragment size of 150 bp using the E210 Covaris plate system (Covaris, Inc. Woburn, MA). The fragmentation settings used were 200 cycles per burst at intensity 4 for 120 seconds. Fragmented DNA was subjected to Illumina DNA sequencing library preparation using a Bravo automated liquid handling platform.

Sequencing libraries were amplified using the bridge-amplification process by Illumina HiSeq pair read cluster generation kits (TruSeq PE Cluster Kit v2.5, Illumina) and were hybridized to custom RNA baits for the Agilent SureSelect protocol. Paired-end, 75 bp sequence reads were generated using Illumina HiSeq 2000 with the target of 1Gb sequence per sample. The sequenced reads were aligned to the reference human genome (NCBI build 37) and deposited in bam format

134 at the European Genome-Phenome Archive (https://www.ebi.ac.uk/ega/, cram files
135 EGAD00001003334, study accession number EGAS00001001223). Additionally, bam files for 93
136 normal samples sequenced with the two panels used in this study were deposited under the
137 accession numbers EGAS00001002124 and EGAS00001001808 (panels V3 and V4,
138 respectively).
139

140 **Bioinformatic Analysis**

141 The breast cancer panels used for DNA capture are described in supplementary data files 1 & 2.
142 They target all coding exons of 366 (first batch) and 280 (second batch) cancer genes that are
143 recurrently mutated, amplified or deleted plus regions showing recurrent copy number variation,
144 and recurrently rearranged introns of fusion genes. The coverage of the first panel is 2028799 bp,
145 that of the second is 2055503 bp, and the overlap is 1089744 bp. Sequencing reads were aligned
146 to the NCBI build 37 human genome using the Burrows-Wheeler Aligner (BWA-aln version 0.5.9, [16]
147 to create BAM files with Smith-Waterman correction [http://bio-bwa.sourceforge.net]. PCR
148 duplicates were marked with biobambam version 2.0.65 [https://github.com/gt1/biobambam2]
149 [17].The tumour samples were compared to 93 FFPE-treated normal samples sequenced with the
150 two panels to an equivalent depth. The sample mean sequencing depth was 574x in batch 1 and
151 787x in batch 2. The mean coverage with 100+ reads was 82% in batch1 and 97% in batch 2.
152 Coverage for individual samples is shown in Sup Fig 2. Variant calling was performed using the
153 Pindel version 4.2 [https://github.com/genome/pindel] and CaVEMan version 1.5.3
154 [https://github.com/cancerit/CaVEMan] algorithms as described [18]. A simple tandem repeat filter
155 was applied first to remove variants observed less than five times or in less than 10% of the reads.
156 Variants present in the normal samples were excluded if the difference in VAF was <0.2. Variants
157 were only considered if observed in both forward and reverse strands. The calls were limited to the
158 regions specified in the panel bed files (sup data 3 & 4). The probes generate sequence up to 50
159 bp on either side of each exon in order to detect splice site mutations. Synonymous mutations in
160 coding regions and variants in UTRs, enhancers and copy number regions are not scored as
161 coding variants. Together with biological selection, for example, counterselection of inactivating
162 mutations in oncogenes, this explains why only 10% of variants are coding mutations. The CNVKit
163 algorithm version 0.9.7b1 was used for copy number segmentation [https://github.com/etal/cnvkit].
164 Unfortunately, the algorithm was unable to fully correct for the lower quality of the FFPE data,
165 leading to batch effects that are visible in the copy number heatmap . To avoid overinterpreting
166 copy number changes we only scored genes as amplified if the affected segment was <15 Mb. For
167 the reported CCND1 amplicons, the median and maximum lengths of the amplified segments were
168 3.3 and 12.8 Mb; for FGFR1 they were 3.5 and 14.6 Mb. To enrich for high-confidence somatic
169 variants, further filtering was performed to remove known constitutional polymorphisms using
170 human variation databases (Ensembl GRCh37, 1000 genomes release 2.2.2 and ESP6500, cut-off

171 VAF ≤0.001); and to remove alterations seen recurrently in the 93 normal DNA samples
172 sequenced with the same protocol. The Variant Allele Fraction was corrected for normal tissue
173 contamination with vafCorrect version 5.4.0 [https://github.com/cancerit/vafCorrect]. Enrichments
174 are defined as variants detected in pre-chemotherapy samples and increased in post-
175 chemotherapy samples. Gains are defined as variants not detected in pre-chemotherapy samples
176 but detected in post-chemotherapy samples. To distinguish between de novo mutations and clonal
177 expansion, coding variants giving VAF = 0 in one sample from a patient were called in both
178 samples without filtering: of the 20 cases where the variant was present in the bam files but
179 removed by the filters, 8 were present once, 3 present twice, 2 present 3 times, 1 present 4 times,
180 2 present 5 times, 2 present 8 times and 2 present 10 times (Sup Table 2). Code availability: Code
181 is available on request to AC or RI.

Results

Demographics, tumour characteristics and treatment of the 42 eligible patients included in this study are given in Sup Table 1. DNA was extracted from frozen biopsies before treatment and from formalin-fixed samples after treatment. It was sequenced in two batches: an initial batch of 17 tumours with single pre-treatment and post-treatment samples; then a second batch including 18 tumours with single pre-treatment and post-treatment samples and 7 tumours with two pre-treatment samples and one post-treatment sample. Thus 91 samples (49 pre-neoadjuvant chemotherapy and 42 post-neoadjuvant chemotherapy) from a total of 42 tumours had evaluable NGS and CNA data.

Mutational landscape

The total number of SNVs and indels in each sample is shown in Sup Fig 3; the median number of variants was 86, with five samples having over 200 variants. As expected, the vast majority of changes in all samples were C>T and G>A substitutions (Sup Fig 4). All three samples from patient PD30315 had a mutation rate much higher than the samples from the other patients. This tumour has an S314A mutation in POLE (DNA polymerase epsilon) that may explain the high mutation rate. It lies in the exonuclease (proofreading) domain and is flanked by known mutations (E311D and D316G, http://mutationaligner.org/domains/PF03104?gene=POLE). It is rare in the EXAC SNP database (8×10^{-5}), and multiple computational predictions score it as pathogenic (DANN, FATHMM, LRT, MutationAssessor and MutationTaster; varsome.com/variant/hg19/rs770403791).

Coding variants

The median number of coding variants (SNVs and indels) per sample was 8, with 2 samples having over 20 coding variants and 12 samples containing less than 5 coding variants (Sup Fig 5). The coding variants in individual genes in each tumour are listed in Sup Table 2. Driver mutations were defined as previously characterised oncogenic mutations [19,20] or mutations that truncate a tumour suppressor protein. The number of tumours with driver mutations in the pre-chemotherapy or post-chemotherapy samples is shown in Fig 1. Seventeen genes had driver mutations in more than one tumour. The commonest genes with driver mutations were PIK3CA (16/42 tumours = 38%), GATA3 (12/42 tumours = 29%), CDH1 (7/42 tumours = 17%), TP53 (7/42 tumours = 17%) and CBFB (5/42 tumours = 12%).

Clonal expansion and contraction after neoadjuvant chemotherapy

The primary objective was to discover mechanisms of resistance to NAC by identifying genetic changes in subclones showing clonal expansion after treatment. To identify subclones showing clonal expansion we compared the VAF in pre- and post-treatment samples (Fig 2a). There were

219 31 putative de novo mutations that appeared after treatment. This was balanced by loss of 30
220 mutations through clonal extinction. These changes affected 46 genes, including 28 driver
221 mutations, in 30 patients. By far the commonest change was PIK3CA mutation but there were
222 changes in both directions: 3 tumours lost mutations, 2 tumours gained them and one tumour had
223 one change in each direction. The next commonest changes were in KMT2C (1 loss, 2 gains) and
224 ARID1A (2 losses, one gain). Examination of the bam files revealed that in 75% of these cases,
225 the variant was actually present at a very low depth when it was called as absent (in two thirds of
226 these cases it was present in one, two or three reads). While it is difficult to draw definitive
227 conclusions from such small numbers of reads, it is likely that in many cases where a new
228 mutation is detected we are seeing expansion of a pre-existing clone rather than a de novo
229 mutation.
230 Fisher tests were used to detect significant changes in VAF that fell short of complete gain or loss.
231 Including the complete gains and losses, 36% of coding variants changed significantly after
232 treatment (Supplementary Table 2, 152/428 variants had $p<0.01$ after Bonferroni correction). Fig
233 2b&c illustrate different patterns of clonal behaviour. In Fig 2b (tumour PD30309) all points lie
234 close to the diagonal, indicating that there was no clonal selection: the cluster at VAF ~0.15
235 represents a tumour subclone whose abundance did not change; the cluster at VAF ~0.5
236 represents either an ancestral tumour clone or heterozygous germline variants that escaped
237 filtering. Consistent with this interpretation, the variants found at VAF ~0.15 are classified as driver
238 mutations in CDH1, PIK3CA, TBX3 and MAP3K1, whereas the variants at VAF ~0.5 are
239 heterozygous missense changes in ACAN, FGFR1, HRNR, PTPN11, RPL5, and WBP1 that are
240 probably either ancestral passenger mutations or rare germline variants. Fig 2c (tumour PD26285)
241 illustrates expansion of a malignant subclone containing CBFB, CDH1 and NF1 driver mutations
242 from a VAF ~0.15 before treatment to a VAF ~0.55 after treatment. The RUNX1 mutation that goes
243 from VAF ~0.15 to ~0.3 is potentially a mutation present initially in the same parental subclone but
244 which failed to expand. Interestingly, RUNX1 is the dimerization partner of CBFB. The CBFB-
245 RUNX1 dimer tethers ER to enhancers; inactivating mutations in either gene could redirect ER to
246 more pernicious targets. Since the subclone containing the CBFB mutation expanded faster it
247 would appear either that the CBFB mutation is better able to inactivate the dimer or perhaps the
248 mutations in CDH1 and NF1 gave the CBFB subclone an added advantage. The remaining
249 variants in this tumour, at VAF ~0.6 before and after treatment, are non-driver mutations in
250 TCF7L2 and TSC1 that could represent passenger mutations or rare germline variants. Similar
251 plots for each individual tumour showing the VAF before and after treatment are presented in Sup
252 Fig 6.
253 Next, instead of looking at all genes in individual tumours, we examined individual genes in
254 all tumours. We give an overview showing the driver oncogenes most frequently mutated before
255 and after treatment in Fig 3a; strikingly, all lie almost perfectly on the diagonal, indicating that none

of these genes is consistently selected for by neoadjuvant chemotherapy. Our interpretation is that they are unlikely to confer resistance to chemotherapy. We can examine the behaviour of individual genes by plotting the VAF for driver mutations in the gene in all tumours (Fig 3b-f). The points represent individual tumours, with the size of the points scaled according to the probability that the VAF changed after treatment. It is immediately obvious that for every gene there are points located far from the diagonal, meaning the clonal abundance changed. Strikingly, there were changes in both directions, meaning driver mutations in a particular gene became more abundant in some tumours and less abundant in others. That clones containing driver oncogenic mutations should become rarer is surprising, particularly for a gene like PIK3CA, but it is important to note that some of the variation may be explained by incomplete correction for the amount of contaminating normal tissue in the samples.

Copy number variants

Copy number changes are plotted in a heatmap in Fig 4a. Gains are shown in red, losses in blue. There are frequent gains of chr1q and chr16p, indicating that the der(1;16) signature translocation of luminal breast cancer was present in most samples. Large chr8q gains, commonly attributed to MYC, were also present in most samples. The most commonly amplified genes were CCND1 (11/42 tumours = 26%) and FGFR1 (11/42 tumours = 26%) (Fig 4b). ERBB2 amplification on chr17 was not seen because tumours with this amplicon were excluded from the study. No fusion genes were detected. Both at the level of the whole genome (Fig 4a), and when individual amplicons were examined (Fig 4b), there were no consistent changes after treatment. There was also no significant difference between the number of breakpoints before and after treatment in the two treatment arms.

Pathway analysis after treatment

In Fig 5 we categorise the driver mutations present after chemotherapy into different functional pathways. The only ESCAT [21] tier IA target is PIK3CA, which has hotspot mutations in 14 tumours. We score the POLE mutation in tumour PD30315 as tier IC, because the tumour has a high mutation burden making it a candidate for immunotherapy. Three tumours had tier IIA PTEN mutations, two tumours had tier IIB AKT1 T17E mutations, two tumours had tier IIIa MDM2 amplification, and one tumour had a tier IIIA somatic BRCA1 mutation. Together, 48% of tumours (20/42) had at least one of these defects. If one adds FGFR1 and CCND1 amplicons, which do not respond to current targeted therapy (tier X), 74% of tumours (31/42) had potentially interesting targets. The remaining mutations in Fig 5 are tier IVA or not in the ESCAT breast cancer list, although many of the latter are targets for preclinical or clinical drugs in other tumour types.

Discussion

293 Our working hypothesis was that clones with recurrent mutations in driver oncogenes would
294 expand after neoadjuvant chemotherapy but we have found no evidence to support it. Since there
295 were multiple changes in VAF and copy number of driver oncogenes after treatment but they show
296 no consistent pattern we conclude that there is no driver oncogene that undergoes strong positive
297 selection under chemotherapy. We confirmed the presence of targetable mutations in many driver
298 oncogenes previously reported to be mutant in breast cancer, and showed that they are not
299 eradicated by neo-adjuvant chemotherapy, but we did not identify any recurrent genetic changes in
300 clones surviving chemotherapy. We therefore conclude that classic mammary oncogenes are
301 probably not responsible for resistance to chemotherapy. This echoes the conclusion from the
302 original EORTC 10994 "p53 study" [15], that p53 status can not be used to select patients for
303 chemotherapy with taxanes. The likely explanation for the negative results in both studies is that
304 chemotherapy targets dividing cells whose rapid division is a distant consequence of the
305 oncogenic mutations that created the tumour. Crucially, the targets of chemotherapy are never
306 mutant in tumours. This contrasts with the paradigm of modern targeted therapy. Pharmacologists
307 will not be surprised by our results: they have long known the metabolic pitfalls that dictate the
308 exposure and response of tumour cells to chemotherapeutic drugs.
309
310 We have confirmed the presence of targetable mutations in many driver oncogenes previously
311 reported to be mutant in pretreatment samples from luminal ER+ breast cancers [10,22,23]. We have
312 shown here that the same mutations are also present in residual disease after chemotherapy. The
313 persistence of classic oncogenic mutations in functionally important pathways in so many tumours
314 after chemotherapy highlights their importance as drug targets. Targeted therapies are either
315 licensed or in development for most of these pathways. ESMO has developed a Scale for Clinical
316 Actionability of molecular Targets (ESCAT) to classify mutations according to the strength of
317 evidence supporting their use in patients with metastatic breast cancer [21]. Tier of evidence IA
318 refers to genetic alterations for which a licensed treatment is known to be effective. The two main
319 contenders are ERBB2 amplification and PIK3CA mutation. PIK3CA was the commonest driver
320 oncogene mutated both before and after chemotherapy in this study. Tumours with ERBB2
321 amplification in the pretreatment samples were excluded from this study, and new ERBB2
322 amplicons were not detected after treatment. Tier IC includes immunotherapy for tumours with a
323 high mutation rate. This is mainly caused by mismatch repair defects but can also result from
324 defective proofreading by the replicative polymerase, DNA polymerase epsilon (POLE). Several
325 tumours had MSH2 mutations of unknown effect. One had a POLE mutation that produced a large
326 increase in the mutation burden, making that tumour an obvious candidate for immunotherapy. Tier
327 II includes gene-drug pairs which have shown activity in breast cancer but for which there is
328 currently no proof that they increase survival in prospective studies. In our data, PTEN loss (IIA)
329 and AKT1 mutation (IIB) fall into this category. Tier III covers gene-drug pairs that show activity in

330 other tumour types, or family members of tier I genes. Two genes fall in this category in our data
331 (BRCA1 and MDM2). The commonest changes we saw are classified as tier IVA, meaning there is
332 good preclinical data to support their exploration in clinical studies. Tier X includes perplexing
333 defects for which treatment should work but does not. It includes CCND1 and FGFR1, the genes
334 most commonly amplified in our study. It is surely only a matter of time before the failure of
335 tumours with these amplicons to respond to ostensibly good drugs is explained, leading to the
336 development of new therapeutic strategies that improve the survival of affected patients. Many of
337 the other mutations in Fig 5 were not assigned a level of evidence because they were not in the 40
338 genes ESMO chose to classify, but effective preclinical or clinical drugs exist for many of them.
339 Mutations in others, like RB1 and FAT1, provide useful information because they confer resistance
340 to licensed drugs. There is thus good reason to be optimistic about the utility of sequencing data,
341 and to foresee an increasing dependence on it in the future. Considering the high risk of relapse of
342 patients with ER+ HER2- tumours with residual disease after NAC, a personalised post NAC
343 strategy based on genomic analysis should be considered a clinical research priority.
344
345 The gene panels we tested cover all currently known mammary oncogenes. The pace of discovery
346 of new oncogenes and tumour suppressor genes in breast cancer has fallen to essentially zero
347 because of the enormous scale of the genomic studies that have already been completed [10,22,23].
348 This means we can confidently exclude the possibility that a common oncogenic driver was
349 missing from the present study. A whole genome sequencing approach would have allowed us to
350 detect mutations in genes that are not known breast cancer genes, but, had we done this without a
351 normal sample to exclude germline variants, the enormous number of unknown variants
352 discovered would have rendered identification of true mediators of resistance a near impossible
353 task. In cases where the mutant fraction for a particular variant changed in one direction in one
354 tumour, there were changes in the opposite direction in other tumours, suggesting that the
355 differences were not caused by clonal selection by the treatment, but only PIK3CA, TP53, GATA3,
356 CDH1 and CBFB were mutant often enough, and CCND1 and FGFR1 amplified often enough, to
357 warrant this type of analysis. This is a recurring theme in genomic studies of breast cancer: many
358 genes are infrequently mutated leading to a multiplicity of tiny groups that defy statistical inference.
359
360 Many drug resistance studies based on clinical trials have produced interesting but inconclusive
361 results [7,8,15,24,25,26]. What is missing is proof that the observed changes play a causal role in drug
362 resistance. To fill this gap requires sophisticated cell biological studies linked to clinical trials.
363 Recent progress in cell culture and xenografting techniques [27-29] mean it is now possible, at least in
364 principle, to perform these studies but the technical challenges are daunting. Specifically, it means
365 establishing cultures of samples taken before treatment, introducing putative genetic changes
366 mediating resistance with viral or CRISPR technology, and showing that the genetically engineered

367 cells acquire the predicted phenotype. Given the risk of sampling artefacts, this should be done
368 with samples containing the broadest possible representation of clones, and with techniques that
369 allow tracing of individual cells in complex mixtures, for example by barcoding the starting material
370 and analysing large numbers of single cells at each step [8].
371
372 In summary, we have performed a targeted sequencing study comparing driver mutations before
373 and after neoadjuvant chemotherapy of luminal breast cancer and found no evidence that
374 expansion of clones containing recurrent driver mutations is responsible for resistance to
375 neoadjuvant chemotherapy. There may be multiple such mechanisms in play, each contributing
376 occasionally to resistance, but new approaches based on functional analysis of material from
377 clinical trials will be required to prove it. Despite our failure to discover new chemotherapy
378 resistance mechanisms, we identified targetable defects both before and after chemotherapy in
379 most of the tumours examined. Future clinical studies should seek to increase the number of
380 licensed drugs available to target these defects
381

Additional information

Acknowledgements

We thank the patients, doctors and nurses involved in the EORTC 10994/BIG 1-00 study for their generous participation. We thank Ultan MacDermott and the Sanger Sample Management and Sequencing team for processing the specimens for NGS.

Authorship

HB, RI and DC conceived the study. DC, HB and EORTC clinical investigators provided clinical samples. CP analysed the clinical data. GMG analysed the histology. JS extracted the DNA. AC and RI analysed the NGS data and made the figures. RI, HB and AC wrote the manuscript. All authors approved the final version of the manuscript and agreed to be accountable for all aspects of the work.

Ethics approval and consent to participate

The EORTC 10994 clinical trial was registered with ClinicalTrials.gov number NCT00017095 and approved by national and/or local ethics committees in all participating centres. Before registration, all patients signed an informed consent for the trial and for mandatory p53 gene assessment on tumour samples. Patients involved in this substudy gave consent for additional biological research on their tumour samples. The study was performed in accordance with the Declaration of Helsinki.

Data availability

Clinical data can be accessed through the EORTC data sharing platform (for details see www.eortc.org/data-sharing). NGS data can be accessed through the European Genome-Phenome Archive (https://www.ebi.ac.uk/ega/, cram files EGAD00001003334, study accession number EGAS00001001223). The NGS data is only accessible under a Managed Access agreement (for details see www.ebi.ac.uk/ega/dacs).

Competing interests

The authors declare no conflict of interest.

Funding information

We thank the Fondation pour la lutte contre le cancer et pour des recherches medico-biologiques, the Site de Recherche Intégrée sur le Cancer – Bordeaux Recherche Intégrée Oncologie Grant INCa-DGOS-Inserm 6046, and the Breast Cancer Working Group EBCC12 grant for financial support. The funding sources had no role in study design, data collection, data analysis, data interpretation, or writing of the report. The corresponding author had full access to all the study

data and the final responsibility for the decision to submit for publication. Trial design, conduct, and analysis were done at the EORTC headquarters, the Institut Bergonié and Wellcome Sanger Institute independently from all funding bodies.

EORTC 10994/BIG 1-00 Consortium (**)

Sophie Abadie-Lacourtoisie (5)
Hervé Bonnefoi (2)
Alexandre Bodmer (6)
Etienne Brain (7)
David Cameron (3)
Tanja Cufer (8)
Mario Campone (9)
Elisabeth Luporsi (10)
Cristian Moldovan (11)
Thierry Petit (12)
Martine Piccart (13)
Franck Priou (14)
Elsbieta Senkus (15)
Khalil Zaman (16)

Affiliations
(2) Institut Bergonié, INSERM U1218, University of Bordeaux, France
(3) University of Edinburgh, Edinburgh, United Kingdom
(5) Centre Paul Papin Institut de Cancérologie de l’Ouest (ICO), Angers, France
(6) Hôpitaux Universitaires de Genève (HUG), Geneva, Switzerland
(7) Institut Curie-Hôpital René Huguenin, Saint-Cloud, France
(8) Tanja Cufer, Institute of Oncology, Ljubljana, Slovenia
(9) Centre René Gauducheau Institut de Cancérologie de l’Ouest (ICO), Nantes, France
(10) Centre Alexis Vautrin, Nancy, France
(11) Centre Henri Becquerel, Rouen, France
(12) Centre Paul Strauss, Strasbourg, France
(13) Institut Jules Bordet, Université Libre de Bruxelles, Brussels, Belgium
(14) Centre Hospitalier de La Roche/Yon, La Roche/Yon, France
(15) Medical University of Gdansk, Gdansk, Poland
(16) Centre Hospitalier Universitaire Vaudois (CHUV), Lausanne, Switzerland

457 **References**

458 1 Cortazar, P., Zhang, L., Untch, M., Mehta, K., Costantino, J. P., Wolmark, N. *et al.*
459 Pathological complete response and long-term clinical benefit in breast cancer: the
460 CTNeoBC pooled analysis. *Lancet* **384**, 164-172 (2014).
461 2 Bonnefoi, H., Litiere, S., Piccart, M., MacGrogan, G., Fumoleau, P., Brain, E. *et al.*
462 Pathological complete response after neoadjuvant chemotherapy is an independent
463 predictive factor irrespective of simplified breast cancer intrinsic subtypes: a landmark and
464 two-step approach analyses from the EORTC 10994/BIG 1-00 phase III trial. *Ann Oncol* **25**,
465 1128-1136 (2014).
466 3 von Minckwitz, G., Untch, M., Blohmer, J. U., Costa, S. D., Eidtmann, H., Fasching, P. A. *et*
467 *al.* Definition and impact of pathologic complete response on prognosis after neoadjuvant
468 chemotherapy in various intrinsic breast cancer subtypes. *J Clin Oncol* **30**, 1796-1804
469 (2012).
470 4 Bonnefoi, H., MacGrogan, G., Poncet, C., Iggo, R., Bergh, J. & Cameron, D. Molecular
471 apocrine tumours in EORTC 10994/BIG 1-00 phase III study: pathological response after
472 neoadjuvant chemotherapy and clinical outcomes. *Br J Cancer* **120**, 913-921 (2019).
473 5 Masuda, N., Lee, S. J., Ohtani, S., Im, Y. H., Lee, E. S., Yokota, I. *et al.* Adjuvant Capecitabine
474 for Breast Cancer after Preoperative Chemotherapy. *N Engl J Med* **376**, 2147-2159 (2017).
475 6 von Minckwitz, G., Huang, C. S., Mano, M. S., Loibl, S., Mamounas, E. P., Untch, M. *et al.*
476 Trastuzumab Emtansine for Residual Invasive HER2-Positive Breast Cancer. *N Engl J Med*
477 **380**, 617-628 (2019).
478 7 Balko, J. M., Giltnane, J. M., Wang, K., Schwarz, L. J., Young, C. D., Cook, R. S. *et al.*
479 Molecular profiling of the residual disease of triple-negative breast cancers after
480 neoadjuvant chemotherapy identifies actionable therapeutic targets. *Cancer Discov* **4**, 232-
481 245 (2014).
482 8 Kim, C., Gao, R., Sei, E., Brandt, R., Hartman, J., Hatschek, T. *et al.* Chemoresistance
483 Evolution in Triple-Negative Breast Cancer Delineated by Single-Cell Sequencing. *Cell* **173**,
484 879-893 e813 (2018).
485 9 Yates, L. R., Gerstung, M., Knappskog, S., Desmedt, C., Gundem, G., Van Loo, P. *et al.*
486 Subclonal diversification of primary breast cancer revealed by multiregion sequencing. *Nat*
487 *Med* **21**, 751-759 (2015).
488 10 TCGA. Comprehensive molecular portraits of human breast tumours. *Nature* **490**, 61-70
489 (2012).
490 11 Bertucci, F., Ng, C. K. Y., Patsouris, A., Droin, N., Piscuoglio, S., Carbuccia, N. *et al.* Genomic
491 characterization of metastatic breast cancers. *Nature* **569**, 560-564 (2019).
492 12 Andre, F., Ciruelos, E., Rubovszky, G., Campone, M., Loibl, S., Rugo, H. S. *et al.* Alpelisib for
493 PIK3CA-Mutated, Hormone Receptor-Positive Advanced Breast Cancer. *N Engl J Med* **380**,
494 1929-1940 (2019).
495 13 Tung, N. M., Robson, M. E., Ventz, S., Santa-Maria, C. A., Nanda, R., Marcom, P. K. *et al.*
496 TBCRC 048: Phase II Study of Olaparib for Metastatic Breast Cancer and Mutations in
497 Homologous Recombination-Related Genes. *J Clin Oncol* 10.1200/JCO.20.02151,
498 JCO2002151 (2020).
499 14 Hyman, D. M., Smyth, L. M., Donoghue, M. T. A., Westin, S. N., Bedard, P. L., Dean, E. J. *et*
500 *al.* AKT Inhibition in Solid Tumors With AKT1 Mutations. *J Clin Oncol* **35**, 2251-2259 (2017).
501 15 Bonnefoi, H., Piccart, M., Bogaerts, J., Mauriac, L., Fumoleau, P., Brain, E. *et al.* TP53 status
502 for prediction of sensitivity to taxane versus non-taxane neoadjuvant chemotherapy in

503 breast cancer (EORTC 10994/BIG 1-00): a randomised phase 3 trial. *Lancet Oncol* **12**, 527-
504 539 (2011).
505 16 Li, H. & Durbin, R. Fast and accurate short read alignment with Burrows-Wheeler
506 transform. *Bioinformatics* **25**, 1754-1760 (2009).
507 17 Tischler, G. & Leonard, S. biobambam: tools for read pair collation based algorithms on
508 BAM files. *Source Code for Biology and Medicine* **9**, 13 (2014).
509 18 Raine, K. M., Hinton, J., Butler, A. P., Teague, J. W., Davies, H., Tarpey, P. *et al.* cgpPindel:
510 Identifying Somatically Acquired Insertion and Deletion Events from Paired End
511 Sequencing. *Curr Protoc Bioinformatics* **52**, 15 17 11-12 (2015).
512 19 Chang, M. T., Asthana, S., Gao, S. P., Lee, B. H., Chapman, J. S., Kandoth, C. *et al.* Identifying
513 recurrent mutations in cancer reveals widespread lineage diversity and mutational
514 specificity. *Nat Biotechnol* **34**, 155-163 (2016).
515 20 Zehir, A., Benayed, R., Shah, R. H., Syed, A., Middha, S., Kim, H. R. *et al.* Mutational
516 landscape of metastatic cancer revealed from prospective clinical sequencing of 10,000
517 patients. *Nat Med* **23**, 703-713 (2017).
518 21 Condorelli, R., Mosele, F., Verret, B., Bachelot, T., Bedard, P. L., Cortes, J. *et al.* Genomic
519 alterations in breast cancer: level of evidence for actionability according to ESMO Scale for
520 Clinical Actionability of molecular Targets (ESCAT). *Ann Oncol* **30**, 365-373 (2019).
521 22 Curtis, C., Shah, S. P., Chin, S. F., Turashvili, G., Rueda, O. M., Dunning, M. J. *et al.* The
522 genomic and transcriptomic architecture of 2,000 breast tumours reveals novel subgroups.
523 *Nature* **486**, 346-352 (2012).
524 23 Nik-Zainal, S., Davies, H., Staaf, J., Ramakrishna, M., Glodzik, D., Zou, X. *et al.* Landscape of
525 somatic mutations in 560 breast cancer whole-genome sequences. *Nature* **534**, 47-54
526 (2016).
527 24 Farmer, P., Bonnefoi, H., Anderle, P., Cameron, D., Wirapati, P., Becette, V. *et al.* A stroma-
528 related gene signature predicts resistance to neoadjuvant chemotherapy in breast cancer.
529 *Nat Med* **15**, 68-74 (2009).
530 25 Quenel-Tueux, N., Debled, M., Rudewicz, J., MacGrogan, G., Pulido, M., Mauriac, L. *et al.*
531 Clinical and genomic analysis of a randomised phase II study evaluating anastrozole and
532 fulvestrant in postmenopausal patients treated for large operable or locally advanced
533 hormone-receptor-positive breast cancer. *Br J Cancer* **113**, 585-594 (2015).
534 26 Weigelt, B., Pusztai, L., Ashworth, A. & Reis-Filho, J. S. Challenges translating breast cancer
535 gene signatures into the clinic. *Nat Rev Clin Oncol* **9**, 58-64 (2011).
536 27 Sachs, N., de Ligt, J., Kopper, O., Gogola, E., Bounova, G., Weeber, F. *et al.* A Living Biobank
537 of Breast Cancer Organoids Captures Disease Heterogeneity. *Cell* **172**, 373-386 (2018).
538 28 Sflomos, G., Dormoy, V., Metsalu, T., Jeitziner, R., Battista, L., Scabia, V. *et al.* A Preclinical
539 Model for ERalpha-Positive Breast Cancer Points to the Epithelial Microenvironment as
540 Determinant of Luminal Phenotype and Hormone Response. *Cancer Cell* **29**, 407-422
541 (2016).
542 29 Richard, E., Grellety, T., Velasco, V., MacGrogan, G., Bonnefoi, H. & Iggo, R. The mammary
543 ducts create a favourable microenvironment for xenografting of luminal and molecular
544 apocrine breast tumours. *J Pathol* **240**, 256-261 (2016).
545

546 **Figure legends**

547

548 **Fig 1. Commonest driver mutations before and after treatment.** The mutation count is non-
549 redundant (ie, genes are only counted once if multiple mutations were identified in a tumour, or the
550 same mutation was present in multiple samples from a tumour).

551

552 **Fig 2. Variants gained and lost after neoadjuvant chemotherapy.** a, Number of coding
553 variants gained and lost in each tumour. b&c, Examples of tumours showing different patterns of
554 clonal change after treatment (b, PD30309, FEC arm; c, PD26285, T-ET arm). The size of the
555 plotting symbol reflects the Fisher p value (mutations supported by fewer reads have a smaller
556 symbol).

557

558 **Fig 3. Frequency and VAF of the most frequently mutated oncogenes and tumour**
559 **suppressor genes before and after neoadjuvant chemotherapy.** a, Percentage of tumours with
560 specific genes mutated before and after treatment. b-f, VAF for the most commonly mutated
561 drivers. There are substantial changes in both directions after treatment. The size of the plotting
562 symbol reflects the Fisher p value (mutations supported by fewer reads have a smaller symbol).

563

564 **Fig 4. Copy number variants in pre- and post-neoadjuvant chemotherapy samples.** a,
565 Heatmap showing regions gained and lost coloured red and blue, respectively. The y axis is
566 ordered by patient ID with pre- followed by post-treatment samples. b, Log2 ratio before and after
567 treatment for the most commonly amplified genes (CCND1 and FGFR1). The dashed grey line
568 corresponds to a copy number of 4. The dotted grey line corresponds to likely gains (3 sd above a
569 copy number of 2). If two pretreatment samples were tested, the second sample is indicated by an
570 X and joined to the first sample by a horizontal line. Note that the FGFR1 sample with log ratio 0.6
571 pre/1.6 post was not scored as amplified because it was not a focal gain. FEC: 5-fluorouracil +
572 epirubicin + cyclophosphamide x6; T-ET: docetaxel x3 then docetaxel + epirubicin x3.

573

574 **Fig 5. Pathway analysis.** Driver oncogenes mutated or amplified after treatment are grouped
575 according to biological pathway. CCND1, FGFR1, AURKA, MDM2 and NCOA3 are within amplified
576 regions; all of the other genes shown contained driver mutations. Note that for amplified regions
577 the true driver may be a nearby gene rather than the one shown.

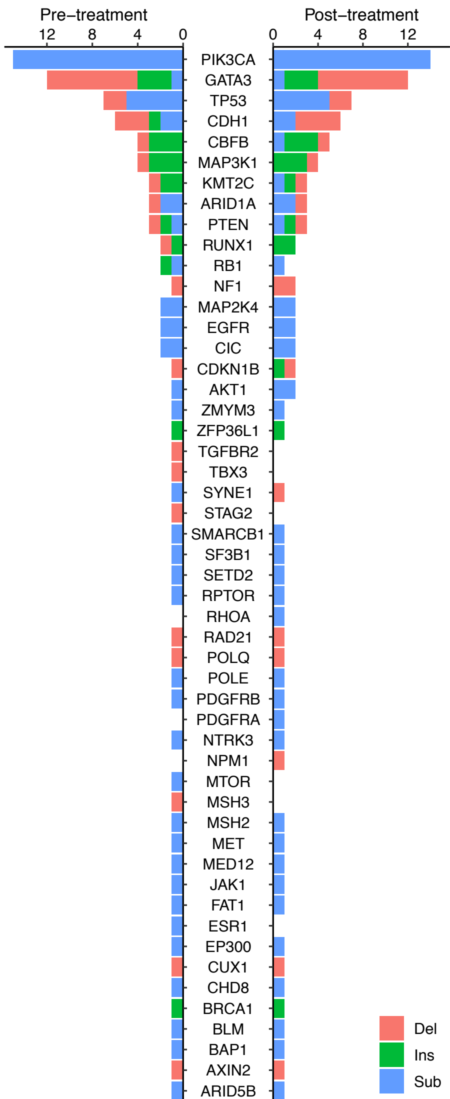

Pre−treatment
Post−treatment
12
8
4
0
0
4
8
12
PIK3CA
GATA3
TP53
CDH1
CBFB
MAP3K1
KMT2C
ARID1A
PTEN
RUNX1
RB1
NF1
MAP2K4
EGFR
CIC
CDKN1B
AKT1
ZMYM3
ZFP36L1
TGFBR2
TBX3
SYNE1
STAG2
SMARCB1
SF3B1
SETD2
RPTOR
RHOA
RAD21
POLQ
POLE
PDGFRB
PDGFRA
NTRK3
NPM1
MTOR
MSH3
MSH2
MET
MED12
JAK1
FAT1
ESR1
EP300
CUX1
CHD8
BRCA1
BLM
BAP1
AXIN2
ARID5B
Del
Ins
Sub

a

Loss | Tumour | Gain

FEC PD30298
FEC PD26286
FEC PD26291
T–ET PD30285
FEC PD26283
T–ET PD30304
FEC PD30299
FEC PD30292
FEC PD26297
T–ET PD30313
T–ET PD30306
T–ET PD30286
FEC PD30325
FEC PD26305
T–ET PD30315
T–ET PD30311
T–ET PD26296
FEC PD30297
T–ET PD30326
T–ET PD30305
T–ET PD26282
T–ET PD26280
FEC PD30327
FEC PD30316
FEC PD26304
FEC PD26288
T–ET PD30302
T–ET PD30284
FEC PD30289
FEC PD26303

3 2 1 0 | 0 1 2 3

Number of variants

b

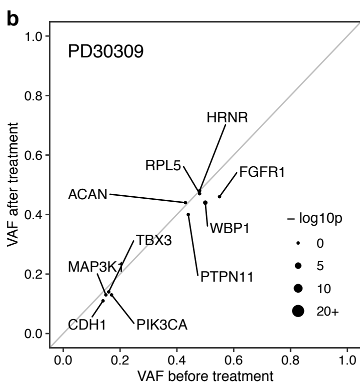

c

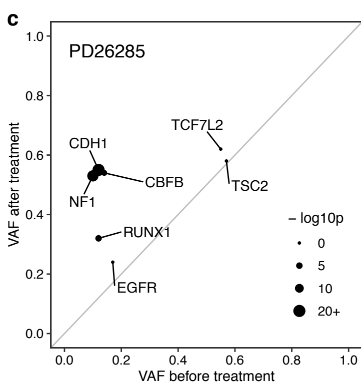

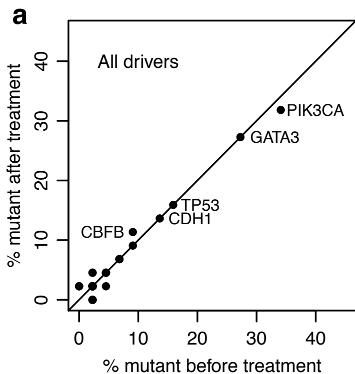
a
All drivers
PIK3CA
GATA3
TP53
CDH1
CBFB
% mutant after treatment
% mutant before treatment
0
10
20
30
40

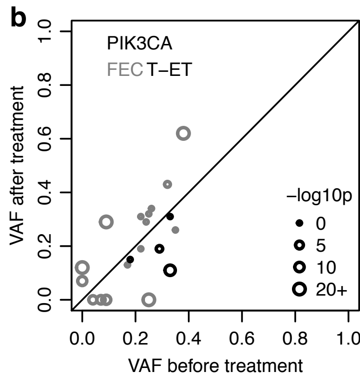
b
PIK3CA
FEC T−ET
−log10p
0
5
10
20+
VAF after treatment
VAF before treatment
0.0
0.2
0.4
0.6
0.8
1.0

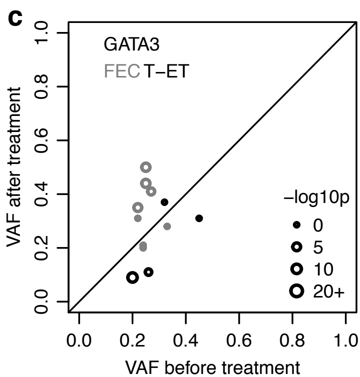
c
GATA3
FEC T−ET
−log10p
0
5
10
20+
VAF after treatment
VAF before treatment
0.0
0.2
0.4
0.6
0.8
1.0

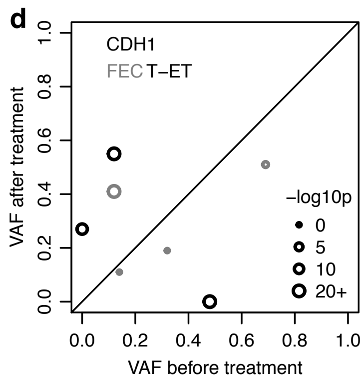
d
CDH1
FEC T−ET
−log10p
0
5
10
20+
VAF after treatment
VAF before treatment
0.0
0.2
0.4
0.6
0.8
1.0

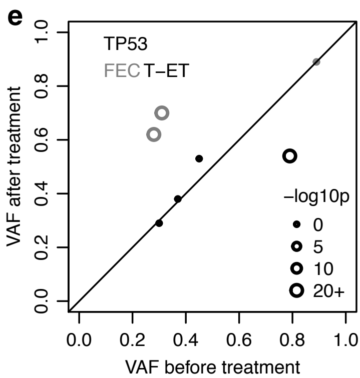
e
TP53
FEC T−ET
−log10p
0
5
10
20+
VAF after treatment
VAF before treatment
0.0
0.2
0.4
0.6
0.8
1.0

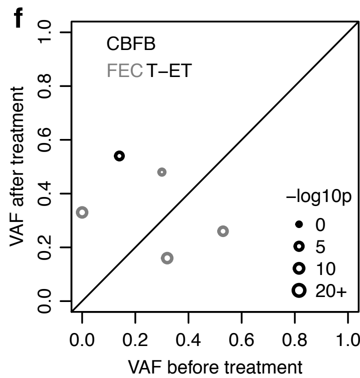
f
CBFB
FEC T−ET
−log10p
0
5
10
20+
VAF after treatment
VAF before treatment
0.0
0.2
0.4
0.6
0.8
1.0

a

PD26305a
PD26305c2
PD26304a
PD26304c2
PD26303a
PD26303c2
PD26302a
PD26302c2
PD26297a
PD26297c2
PD26296a
PD26296c2
PD26292a
PD26292c2
PD26291a
PD26291c2
PD26290a
PD26290c2
PD26289a
PD26289c2
PD26288a
PD26288c2
PD26286a2
PD26286c2
PD26285a
PD26285c2
PD26283a
PD26283c2
PD26282a
PD26282c
PD26281a
PD26281c2
PD26280a
PD26280c2
PD30327c
PD30327a
PD30326c
PD30326a
PD30325c
PD30325a
PD30324c
PD30324a
PD30319c
PD30319a
PD30318c
PD30318a
PD30316c
PD30316a
PD30315c
PD30315a
PD30314c
PD30314a
PD30313c
PD30313a
PD30311c
PD30311a
PD30309c
PD30309a
PD30307c
PD30307a
PD30306c
PD30306a
PD30305c
PD30305a
PD30304c
PD30304a
PD30302c
PD30302a
PD30299c
PD30299a
PD30298c
PD30298a
PD30297c
PD30297a
PD30292c
PD30292a
PD30289c
PD30289a
PD30286c
PD30286a
PD30285c
PD30285a
PD30284c
PD30284a

1 2 3 4 5 6 7 8 9 10 11 12 13 14 15 16 17 18 19 20 21 22 X

log2: 1, 0, −1

b

CCND1
FEC T−ET
log2 ratio before treatment
log2 ratio after treatment

FGFR1
FEC T−ET
log2 ratio before treatment
log2 ratio after treatment

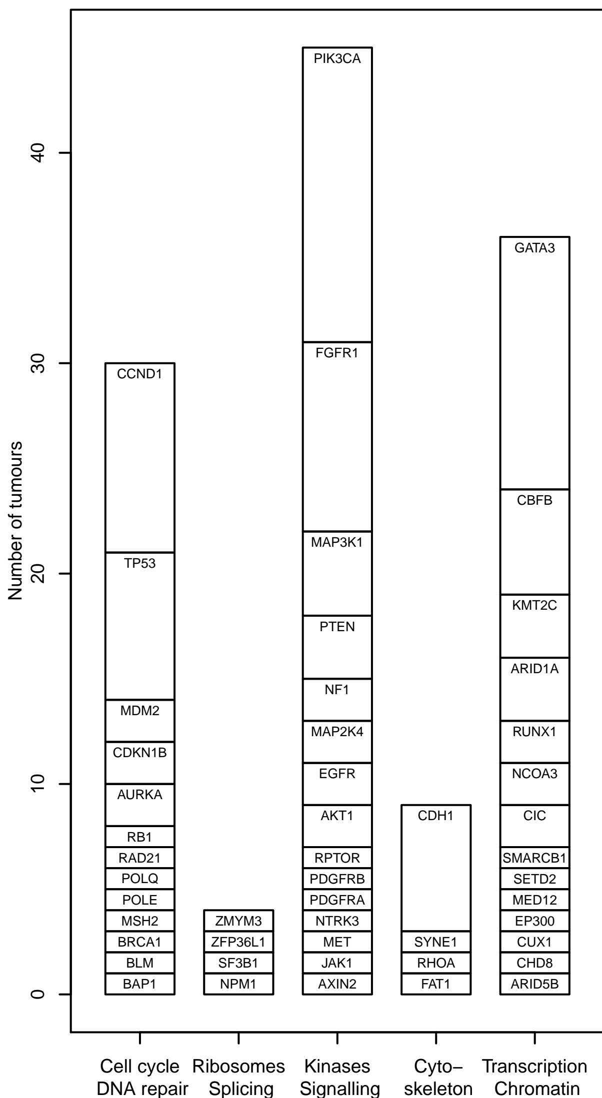
Number of tumours
0
10
20
30
40
CCND1
TP53
MDM2
CDKN1B
AURKA
RB1
RAD21
POLQ
POLE
MSH2
BRCA1
BLM
BAP1
ZMYM3
ZFP36L1
SF3B1
NPM1
PIK3CA
FGFR1
MAP3K1
PTEN
NF1
MAP2K4
EGFR
AKT1
RPTOR
PDGFRB
PDGFRA
NTRK3
MET
JAK1
AXIN2
CDH1
SYNE1
RHOA
FAT1
GATA3
CBFB
KMT2C
ARID1A
RUNX1
NCOA3
CIC
SMARCB1
SETD2
MED12
EP300
CUX1
CHD8
ARID5B
Cell cycle DNA repair
Ribosomes Splicing
Kinases Signalling
Cyto– skeleton
Transcription Chromatin